Predictive Control Algorithm for Speed and Displacement Tracking of Urban Rail Trains

Xi Wang, Kejia Xing*, Jian Wang, and Wei Zheng

***Abstract*—This paper proposes a predictive control algorithm for the speed and displacement tracking of urban rail trains. Firstly, the train dynamics model is constructed considering the resistance existing in the actual operational scenarios. Secondly, based on the model predictive control (MPC) framework, a control objective function for tracking the desired speed and displacement and the stable change of control quantities is designed. Finally, combined with constraints of the train operation, the proposed MPC algorithm for the train tracking control problem is transformed into quadratic programming with inequality constraints, thereby facilitating a solution with the commonly-used solvers. Experimental results demonstrate that the proposed algorithm can effectively enhance the speed and displacement control performance while improving energy efficiency, ensuring the safety, stability, and riding comfort of the train.**

***Index Terms*—Automatic train operation (ATO), urban rail train (URT), train speed and displacement control, and model predictive control (MPC).**

I. Introduction

THE speed and displacement tracking control of urban rail trains (URTs) is crucial in automatic train operation (ATO) [1], [2], [3]. As the urban rail transit evolves, traditional speed and displacement tracking control algorithms may not adequately meet the real-world demands. Therefore, to enhance the overall performance of the URT, it is imperative to design an effective ATO control algorithm to achieve safe, smooth, and efficient speed and displacement tracking, ensuring the punctuality, riding comfort, and energy efficiency of the train operation.

Because the resistance of the multi-carriage train running on the urban rail is lower than the traction and braking force, it is generally simplified as a single-point model, and its longitudinal motion is approximated by Newton equation [4]. This model has been widely used in the ATO control technology for urban rail transit systems [5]. For example, Albrecht et al. [6] presents a versatile train control model that explores the energy-efficient control strategy for trains within the stipulated travel time. Furthermore, Lian et al. [7] devise a speed control algorithm based on the single-point model which can effectively enhance the anti-interference ability and minimize the tracking error.

Notice that, there are lots of factors that may potentially affect the performance of URTs, such as the motor saturation characteristics, riding comfort, constraints on the train speed, and the station stopping position. Therefore, the design of control algorithms necessitates careful consideration of both control objectives and constraints. Traditionally, the proportional-integral-derivative (PID) control [8], [9], [10] and slide mode control (SMC) [11], [12] are widely employed in the URT for speed and displacement tracking control, which boast simplicity in implementation and stability. Nevertheless, the aforementioned control algorithms cannot concurrently optimize multiple objectives and constraints [13], [14]. Given these limitations, the model predictive control (MPC) method has garnered significant attention in recent years for its effectiveness in addressing complex optimization control problems and diverse constraints [15], [16], [17]. Zhang et al. [18] present an MPC algorithm incorporating multiple performance indicators and constraints while introducing two penalty factors to reduce energy wastage and mitigate train cycle vibrations. In [19], an MPC algorithm based on constraint tightening is devised, enabling speed tracking close to, but not exceeding the automatic train protection (ATP) profile. Zhang et al. [20] introduce a switching MPC algorithm, where the cost function in train control problems is adjusted based on train operational requirements. Notably, these MPC algorithms rely on train traction/braking outputs for the speed control and do not incorporate variations in traction/braking outputs related to the riding comfort. Hence, using control input increments is essential for the URT to achieve smooth, safe, and precise control of the speed and displacement tracking.

In this paper, a predictive control algorithm based on control input increment level is proposed for the ATO of the URT. This approach achieves precise speed and displacement tracking control for the URT during inter-station travel and satisfies punctuality, riding comfort, and energy efficiency in real-world scenarios. The structure of this paper is as follows: Section II delineates the formulation of a predictive control model for train speed and displacement. Section III is dedicated to the meticulous design of objective functions governing the speed and displacement tracking control. Section IV meticulously crafts the constraints of the ATO. Section V presents simulation outcomes along with their corresponding analyses. In Section VI, we conclude the whole paper. The framework of the predictive control algorithm for the speed and displacement tracking of URTs is shown in Fig. 1.

The contributions of this paper can be summarized as follows:

1) This paper introduces the traction/braking control input

Manuscript received December 23, 2023; revised May 18, 2024. This work was supported in part by the National Natural Science Foundation of China under Grant 52172323; and in part by the China Academy of Railway Sciences Fund under Grant 2021YJ305.

Xi Wang is a Ph.D. candidate at the China Academy of Railway Sciences, Beijing, China, 100081. (e-mail: wangxcars@163.com).

Kejia Xing is a Researcher at the Signal and Communication Research Institute, China Academy of Railway Sciences Corporation Ltd., Beijing, China, 100081. (Corresponding author to provide phone: 18847700177; e-mail: xingkejia@rails.cn).

Jian Wang is an Associate Researcher at Signal and Communication Research Institute, China Academy of Railway Sciences Corporation Ltd., Beijing, China, 100081. (e-mail: tim21wang@163.com).

Wei Zheng is an Associate Researcher at Signal and Communication Research Institute, China Academy of Railway Sciences Corporation Ltd., Beijing, China, 100081. (e-mail: zhengwei209222@163.com).

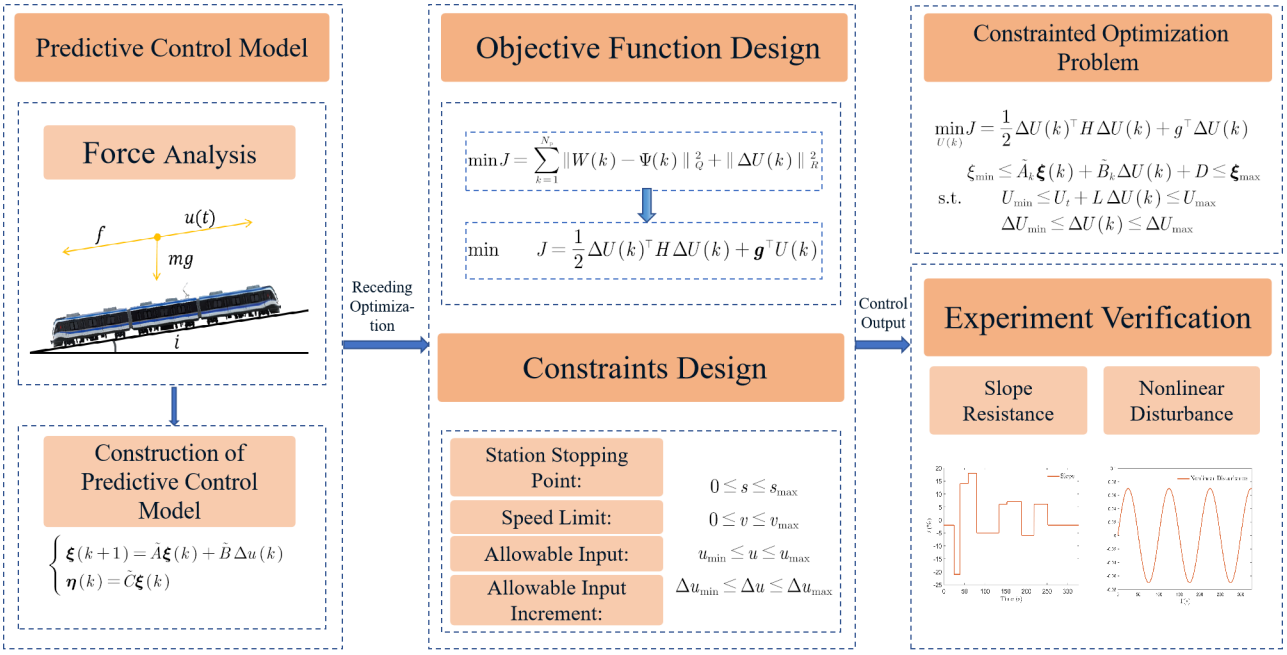

Fig. 1: Framework of the predictive control algorithm for urban rail trains.

increments into the existing train dynamics model, aiming to prevent excessive changes in traction and braking forces. Simultaneously, considering the slope resistance during the train operation, a single-point dynamics model for the URT is established. This model not only ensures the precise tracking of train speed and displacement but also incorporates the riding comfort and additional slope resistance.

2) Taking into account various inter-station operational scenarios for the URT, this paper formulates the tracking performance of the desired speed and displacement profiles and the smoothness of control inputs, as control objectives. These objectives are transformed into quadratic forms and integrated with constraints such as the station stopping position, speed limitation, and traction/braking control increments.
3) The experimental results demonstrate the superior ability of the proposed algorithm to track the desired speed and displacement profiles, reducing errors of the speed and displacement, and possessing excellent anti-disturbance performance.

II. Predictive Control Model For Train Speed and Displacement

During the train operation, it is subject to the collective influence of the traction, braking, and resistance. Therefore, the dynamics equations for a train can be articulated as follows:

$$\dot{s}(t) = v(t), m\dot{v}(t) = ma(t) = u(t) - f, \tag{1}$$

where $v(t)$ represents the speed of the train; $s(t)$ denotes the position of the train; m signifies the mass of the train; $a(t)$ represents the acceleration of the train; $u(t)$ represents the traction force acting on the train. f stands for the resistance, which specifically includes $f = f_{\mathrm{r}} + f_{\mathrm{w}}$; f_{r} is the basic resistance correlated with speed; f_{w}, the additional resistance related to track conditions, encompass slope resistance, tunnel resistance, and curve resistance [21]. The force condition of the URT is illustrated in Fig. 2.

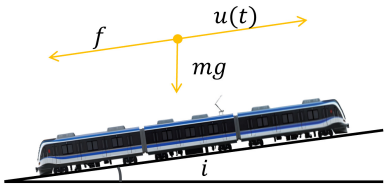

Fig. 2: Force condition of the urban rail train.

In the ATO system for the URT, train control solely considers the impact of basic resistance and slope resistance on the train. The resistances experienced by the train are formulated as follows:

$$f_{\mathrm{r}} = a + bv + cv^2, \tag{2}$$

$$f_{\mathrm{w}} = m \cdot g \cdot i \cdot 10^{-3}. \tag{3}$$

Equation (2) presents the formula for calculating basic operational resistance, where a, b, and c denote basic resistance coefficients, respectively. Equation (3) represents the computation of slope resistance, where g is the acceleration due to gravity, and i represents the slope in percentage (positive for uphill) [22]. Upon simplifying (1), we derive

$$\begin{cases} \dot{s}(t) = v(t), \\ \dot{v}(t) = a(t) = \frac{u(t)}{m} - \frac{f}{m}. \end{cases} \tag{4}$$

By substituting (2) and (3) into (4), we obtain

$$\begin{cases} \dot{s}(t) = v(t), \\ \dot{v}(t) = \frac{u(t)}{m} - \frac{a+bv(t)+cv^2(t)+f_{\mathrm{w}}}{m}. \end{cases} \tag{5}$$

Given the presence of higher-order terms concerning the speed, a first-order Taylor approximation of $v(t)$ around $v_{\mathrm{r}}(t)$

is performed using linearization methods [23], where $v_{\mathrm{r}}(t)$ represents the reference speed of the train, leading to

$$f(v(t)) \approx f\left(v_{\mathrm{r}}(t)\right)+\frac{\mathrm{d}f\left(v_{\mathrm{r}}(t)\right)}{\mathrm{d}v_{\mathrm{r}}(t)}\left(v(t)-v_{\mathrm{r}}(t)\right). \quad (6)$$

Further, we obtain

$$\begin{cases} \dot{s}(t)=v(t), \\ \dot{v}(t)=\frac{u(t)}{m}-\frac{[b+2v_{\mathrm{r}}(t)c]v(t)}{m}+\frac{\left(cv_r(t)^2-a-f_{\mathrm{w}}\right)}{m}. \end{cases} \quad (7)$$

Substituting this approximation into the dynamics equation, we acquire the linearized state-space representation of the train motion system, expressed as

$$\begin{cases} \dot{\boldsymbol{x}}(t)=A\boldsymbol{x}(t)+Bu(t)+\boldsymbol{d}, \\ \boldsymbol{y}(t)=C\boldsymbol{x}(t), \end{cases} \quad (8)$$

where $\boldsymbol{x}=[s(t);v(t)]$,

$$A=\begin{bmatrix} 0 & 1 \\ 0 & -\frac{b+2v_{\mathrm{r}}(t)c}{m} \end{bmatrix}, \quad B=\begin{bmatrix} 0 \\ \frac{1}{m} \end{bmatrix},$$

$$C=\begin{bmatrix} 1 & 0 \\ 0 & 1 \end{bmatrix}, \quad \boldsymbol{d}=\begin{bmatrix} 0 \\ \frac{\left(cv_{\mathrm{r}}^2(t)-a-f_{\mathrm{w}}\right)}{m} \end{bmatrix}.$$

Applying discretization to (8), one has

$$\begin{cases} \boldsymbol{x}(k+1)=A_{\mathrm{d}}\boldsymbol{x}(k)+B_{\mathrm{d}}u(k), \\ \boldsymbol{y}(k)=C_{\mathrm{d}}\boldsymbol{x}(k), \end{cases} \quad (9)$$

where $A_{\mathrm{d}}=I+AT, B_{\mathrm{d}}=TB, C_{\mathrm{d}}=C$, and I represents the identity matrix and T signifies the sampling period.

Furthermore, considering the riding comfort, this paper introduces a new state vector $\boldsymbol{\xi}(k)=[\boldsymbol{x}(k);u(k-1)]$. (9) can be rewritten as a state equation with control input increments [24], [25]:

$$\begin{cases} \boldsymbol{\xi}(k+1)=\tilde{A}\boldsymbol{\xi}(k)+\tilde{B}\Delta u(k), \\ \boldsymbol{\eta}(k)=\tilde{C}\boldsymbol{\xi}(k), \end{cases} \quad (10)$$

where

$$\tilde{A}=\begin{bmatrix} A_{\mathrm{d}} & B_{\mathrm{d}} \\ O_{1\times 2} & 1 \end{bmatrix}, \tilde{B}=\begin{bmatrix} B_{\mathrm{d}} \\ 1 \end{bmatrix}, \tilde{C}=\begin{bmatrix} C_{\mathrm{d}} & O_{2\times 1} \\ O_{1\times 2} & 0 \end{bmatrix}.$$

In the above expression, O denotes the zero matrix with the appropriate dimension. Based on (10), for state prediction, let N_{c} represent the control domain and N_{p} denotes the prediction domain, thereby simplifying them into a compact form:

$$\Xi(k)=F_{\xi}\boldsymbol{\xi}(k)+G_{\xi}\Delta U(k), \quad (11)$$

where

$$\Xi(k)=\begin{bmatrix} \boldsymbol{\xi}(k+1) \\ \vdots \\ \boldsymbol{\xi}\left(k+N_{\mathrm{p}}\right) \end{bmatrix}, \Delta U(k)=\begin{bmatrix} \Delta u(k) \\ \vdots \\ \Delta u\left(k+N_{\mathrm{p}}-1\right) \end{bmatrix},$$

$$F_{\xi}=\begin{bmatrix} \tilde{A} \\ \vdots \\ \tilde{A}^{N_{\mathrm{p}}} \end{bmatrix}, G_{\xi}=\begin{bmatrix} \tilde{B} & & 0 \\ \vdots & \ddots & \\ \tilde{A}^{N_{\mathrm{p}}-1}\tilde{B} & \cdots & \tilde{B} \end{bmatrix}.$$

Incorporating the output equation from (10) and (11), we derive

$$\Psi(k)=F_{\eta}\boldsymbol{\xi}(k)+G_{\eta}\Delta U(k), \quad (12)$$

where

$$\Psi(k)=\begin{bmatrix} \boldsymbol{\eta}(k+1) \\ \vdots \\ \boldsymbol{\eta}\left(k+N_{\mathrm{p}}\right) \end{bmatrix}, F_{\eta}=\begin{bmatrix} \tilde{C}\tilde{A} \\ \vdots \\ \tilde{C}\tilde{A}^{N_{\mathrm{p}}} \end{bmatrix},$$

$$G_{\eta}=\begin{bmatrix} \tilde{C}\tilde{B} & & 0 \\ \vdots & \ddots & \\ \tilde{C}\tilde{A}^{N_{\mathrm{p}}-1}\tilde{B} & \cdots & \tilde{C}\tilde{A}^{N_{\mathrm{p}}-N_{\mathrm{c}}}\tilde{B} \end{bmatrix}.$$

III. Objective Function Design

The objective function of this paper is to ensure the rapid and smooth tracking of the desired trajectory. Therefore, the overarching control goals are speed and displacement of the train, incorporating optimization of deviations in system state variables and control inputs. Simultaneously, to consider the riding comfort and avoid excessive traction/braking changes, the design of the objective function is formulated as

$$J=\sum_{k=1}^{N_{\mathrm{p}}}\|W(k)-\Psi(k)\|_Q^2+\sum_{k=1}^{N_{\mathrm{c}}}\|\Delta U(k)\|_R^2, \quad (13)$$

where $W(k)=\left[\mathbf{w}_{\mathrm{r}}(k+1)\ldots\mathbf{w}_{\mathrm{r}}(k+N_{\mathrm{p}})\right]$. represents the vector representation of the desired output values, and Q and R are weighting matrices with appropriate dimensions [26]. The first term on the right-hand side of (13) reflects the system's ability to track the desired trajectory. The second term represents the requirement for smooth variations in control inputs.

Quadratic programming is widely used in the field of the MPC [27]. Therefore, this paper further transforms the objective function in (13) into quadratic programming. First, let $E=F_{\eta}\xi(k)$ and substitute (12) into the optimization objective in (13), and we obtain

$$\begin{aligned} J&=(W(k)-\Psi(k))^{\top}\tilde{Q}(W(k)-\Psi(k))+\Delta U(k)^{\top}\tilde{R}\Delta U(k) \\ &=\Delta U(k)^{\top}\left(G_{\eta}^{\top}\tilde{Q}G_{\eta}+\tilde{R}\right)\Delta U(k) \\ &+2\left[E^{\top}\tilde{Q}G_{\eta}-W(k)^{\top}\tilde{Q}G_{\eta}\right]\Delta U(k) \\ &+W(k)^{\top}\tilde{Q}W(k)-2W(k)^{\top}\tilde{Q}E+E^{\top}\tilde{Q}E. \end{aligned} \quad (14)$$

In these equations, $\tilde{Q}=I_{N_{\mathrm{p}}}\otimes Q$ and $\tilde{R}=I_{N_{\mathrm{c}}}\otimes R$, where $\otimes$ represents the Kronecker product. Neglecting the constant term in (14), and one has

$$\begin{aligned} J&=\Delta U(k)^{\top}\left(G_{\eta}^{\top}\tilde{Q}G_{\eta}+\tilde{R}\right)\Delta U(k) \\ &+2\left[E^{\top}\tilde{Q}G_{\eta}-W(k)^{\top}\tilde{Q}G_{\eta}\right]\Delta U(k). \end{aligned} \quad (15)$$

Let $H={G_{\eta}}^{\top}\tilde{Q}G_{\eta}+\tilde{R}$, and $\boldsymbol{g}={G_{\eta}}^{\top}\tilde{Q}\left[E-W(k)\right]$, then (15) can be rearranged as

$$J=\frac{1}{2}\Delta U(k)^{\top}H\Delta U(k)+\boldsymbol{g}^{\top}U(k). \quad (16)$$

IV. Constraints Design

The URT needs to arrive at the target station within the specified time and remain aligned with the platform screen door [28]. Therefore, the position constraint for the train at the target station is designed as

$$0\le s(k)\le s_{\max}, \quad (17)$$

where $s_{\max}$ represents the stopping position of the train at the station.

The speed of the train operation is constrained by the maximum allowable speed of the track conditions, the speed limits imposed by the ATP profile, and the restrictions based on the maximum safe operating speed [29]. In this regard, the speed constraint for the train is expressed as

$$0 \le v(k) \le v_{\max}, \tag{18}$$

where $v_{\max} = \min\{v_{\mathrm{l}}, v_{\mathrm{p}}, v_{\mathrm{t}}\}$, v_{l} is the maximum allowable speed determined by track conditions, v_{p} is the speed limit from the ATP profile, and v_{t} is the maximum safe operating speed of the URT.

The maximum traction/braking force under the influence of the saturation characteristics of the train traction motors is constrained as

$$u_{\min} \le u(k) \le u_{\max}, \tag{19}$$

where $u_{\min}$ and $u_{\max}$ respectively represent the output thresholds for maximum traction/braking force achievable due to the physical limitations of the traction motors.

To ensure the riding comfort, it is necessary to impose constraints on the variation of traction/braking force, as outlined below

$$\Delta u_{\min} \le \Delta u(k) \le \Delta u_{\max}, \tag{20}$$

where $\Delta u_{\max}$ represents the maximum allowable change in traction force, and $\Delta u_{\min}$ represents the maximum allowable change in braking force.

In the objective function, as the control input increments within the control horizon are taken as the decision variables to be solved, it is necessary to transform the constraint conditions into the form of control input increments. The aforementioned constraints in (17)-(20) can be rearranged as

$$\boldsymbol{\xi}_{\min} \le Z\boldsymbol{\xi}(k+1+i) \le \boldsymbol{\xi}_{\max}, \tag{21}$$

$$u_{\min} \le u(k+i) \le u_{\max}, \tag{22}$$

$$\Delta u_{\min} \le \Delta u(k+i) \le \Delta u_{\max}, \tag{23}$$

where $i = 0, 1, \cdots, N-1$. Z ensures that the constraints on train displacement and train speed, with $Z = \begin{bmatrix}1 & 0 & 0; 0 & 1 & 0\end{bmatrix}$. $\boldsymbol{\xi}_{\min}$ represents the minimum values for train displacement and train speed, defined as $\boldsymbol{\xi}_{\min} = \begin{bmatrix}0 & 0\end{bmatrix}^{\top}$. $\boldsymbol{\xi}_{\max}$ represents the maximum values for train displacement and train speed, defined as $\boldsymbol{\xi}_{\max} = \begin{bmatrix}s_{\max} & v_{\max}\end{bmatrix}^{\top}$.

Within the prediction horizon, as indicated by (19), the constraint can be represented as

$$\boldsymbol{\xi}_{\min} \le \tilde{A}_k\boldsymbol{\xi}(k) + \tilde{B}_k\Delta U(k) + D \le \boldsymbol{\xi}_{\max}, \tag{24}$$

where

$$\tilde{A}_k = \begin{bmatrix} Z\tilde{A}; & Z\tilde{A}^2; & \cdots & ; Z\tilde{A}^{N_{\mathrm{p}}} \end{bmatrix},$$

$$D = \begin{bmatrix} \boldsymbol{d}; & \boldsymbol{d}; & \cdots; & \boldsymbol{d} \end{bmatrix}^{\top},$$

$$\tilde{B}_k = \begin{bmatrix} Z\tilde{B} & 0 & \cdots & 0 \\ Z\tilde{A}\tilde{B} & Z\tilde{B} & \ddots & \vdots \\ \vdots & \vdots & \ddots & 0 \\ \tilde{A}^{N_{\mathrm{p}}-1}\tilde{B} & Z\tilde{A}^{N_{\mathrm{p}}-2}\tilde{B} & \cdots & Z\tilde{A}^{N_{\mathrm{p}}-N_{\mathrm{c}}}\tilde{B} \end{bmatrix}.$$

The relationship between control inputs and control input increments is shown as

$$u(k+i) = u(k+i-1) + \Delta u(k+i),$$
$$i = 0, 1, \cdots, N-1.$$

Equation (23) can be represented in vector form as

$$U_{\min} \le U_t + L\Delta U(k) \le U_{\max}, \tag{25}$$

where $U_t = \mathbf{1}_{N_{\mathrm{c}}} \otimes u(k-1)$,

$$L = \begin{bmatrix} \mathbf{1} & & \\ \vdots & \ddots & \\ \mathbf{1} & \cdots & \mathbf{1} \end{bmatrix}_{N_{\mathrm{c}} \times N_{\mathrm{c}}}.$$

$\mathbf{1}_{N_{\mathrm{c}}}$ is a column vector containing N_{c} rows, where all elements are 1; $u(k-1)$ represents the actual control inputs at the previous time step. $U_{\min}$ and $U_{\max}$ are the sets of minimum and maximum values for control inputs within the control horizon, respectively. The constraint on control input increments can be represented as

$$\Delta U_{\min} \le \Delta U(k) \le \Delta U_{\max}, \tag{26}$$

where $\Delta U_{\min}$ and $\Delta U_{\max}$ represent the sets of minimum and maximum values for control input increments within the control horizon.

Finally, the constrained optimization problem regarding the train speed and displacement can be transformed into quadratic programming:

$$\begin{aligned} \min_{U(k)} J &= \frac{1}{2}\Delta U(k)^{\top} H \Delta U(k) + g^{\top}\Delta U(k) \\ &\xi_{\min} \le \tilde{A}_k\boldsymbol{\xi}(k) + \tilde{B}_k\Delta U(k) + D \le \boldsymbol{\xi}_{\max} \\ \text{s.t.} \quad & U_{\min} \le U_t + L\Delta U(k) \le U_{\max} \\ & \Delta U_{\min} \le \Delta U(k) \le \Delta U_{\max} \end{aligned} \tag{27}$$

After solving the optimization problem within each control cycle with existing solvers, such as the 'Quadprog' function in Matlab, a series of the control input increments within the control horizon is obtained

$$\Delta U^*(k) = \begin{bmatrix} \Delta u^*(k) \\ \Delta u^*(k+1) \\ \cdots \\ \Delta u^*\left(k+N_{\mathrm{c}}-1\right) \end{bmatrix}.$$

The first element of this control sequence is applied as the actual control input increment to the system, i.e.,

$$u(k) = u(k-1) + \Delta u^*(k).$$

Upon entering the next control cycle, the above process is repeated, thus cyclically achieving tracking control of the train's speed and displacement trajectory.

V. Experiment Verification

The data used in this paper is sourced from operational data from a specific urban rail line. Further, an 8-carriage train composition is chosen, employing a D-Type train model, with specific parameters provided by the vehicle manufacturer, as shown in Table I. It is assumed that the speed and displacement information of the train is obtained through sensors, and the actuators are considered to be healthy and free of faults.

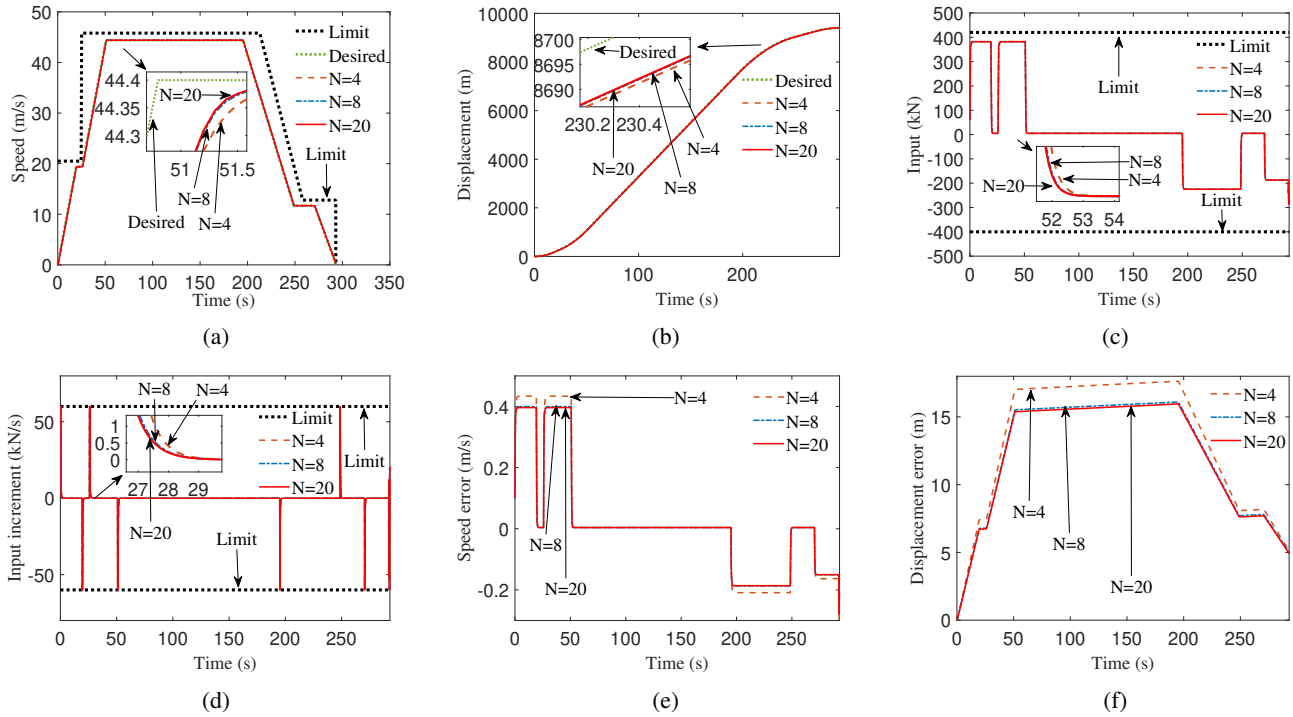

Fig. 3: Comparison of performance in different horizons.

This paper verifies the algorithm's performance through the following experiments: (1) The experiment of the MPC algorithm in different horizons. (2) The comparative experiment of different algorithms without slope resistance. (3) The comparative experiments of different algorithms with slope resistance. (4) The comparative experiments of different algorithms with the nonlinear disturbance.

TABLE I: Parameters of train

Parameters	Value
m (t)	378
a (N/t)	9.888
b (Ns/mt)	0.005
c ($\mathrm{Ns^2/m^2t}$)	0.00195
$u_{\max}$ (kN)	420
$u_{\min}$ (kN)	400
$\Delta u_{\max}$ (kN/s)	60
$\Delta u_{\min}$ (kN/s)	60

In particular, we specify the commonly used indicators to evaluate the performance of the control algorithm, described as follows [2]:

1) Punctuality: Punctuality is defined as the error between the actual speed and displacement of the train and the desired speed and displacement. The smaller the speed and displacement errors, the better the punctuality of the ATO control algorithm. The specific formula is as follows:

$$\mathrm{E}_v = \frac{\sum_{k=0}^{T} |v_{\mathrm{r}}(k) - v(k)|}{T},$$

$$\mathrm{E}_s = \frac{\sum_{k=0}^{T} |s_{\mathrm{r}}(k) - s(k)|}{T},$$

where E_v represents the average speed error and E_s represents the average displacement error.

2) Riding comfort: The average change of the control input increment can be used to evaluate the riding comfort of the train operation process. As long as the control input increment does not exceed the limits, it can be considered that the ATO control algorithm can meet the riding comfort.
3) Energy efficiency: We consider the energy consumption generated during the traction and braking process of the train, without considering the energy consumption of basic equipment, and one has

$$\mathrm{E}_u = \int u^2 dt,$$

where E_u represents input cost. The greater the input cost, the lower the energy efficiency.

A. Experiment Verification in Different Horizons

For this simulation, 4, 8, and 20 are chosen for the prediction and control horizons, respectively. The effectiveness of the control algorithm is validated while keeping other weight parameters unchanged. The output and control weighting matrix parameters are denoted as Q and R, respectively.

Figure 3(a) illustrates the comparison of train speed control performance under different prediction horizons and control horizons while ensuring compliance with the maximum safe operating speed requirement. The thicker black dashed line represents the speed limit curve, with a maximum speed limit of 45.8 m/s. From Fig. 3(a), it is evident that the actual speed under different horizons can accurately track the desired speed profile. As the prediction and control horizons increase, the speed-tracking effectiveness improves significantly.

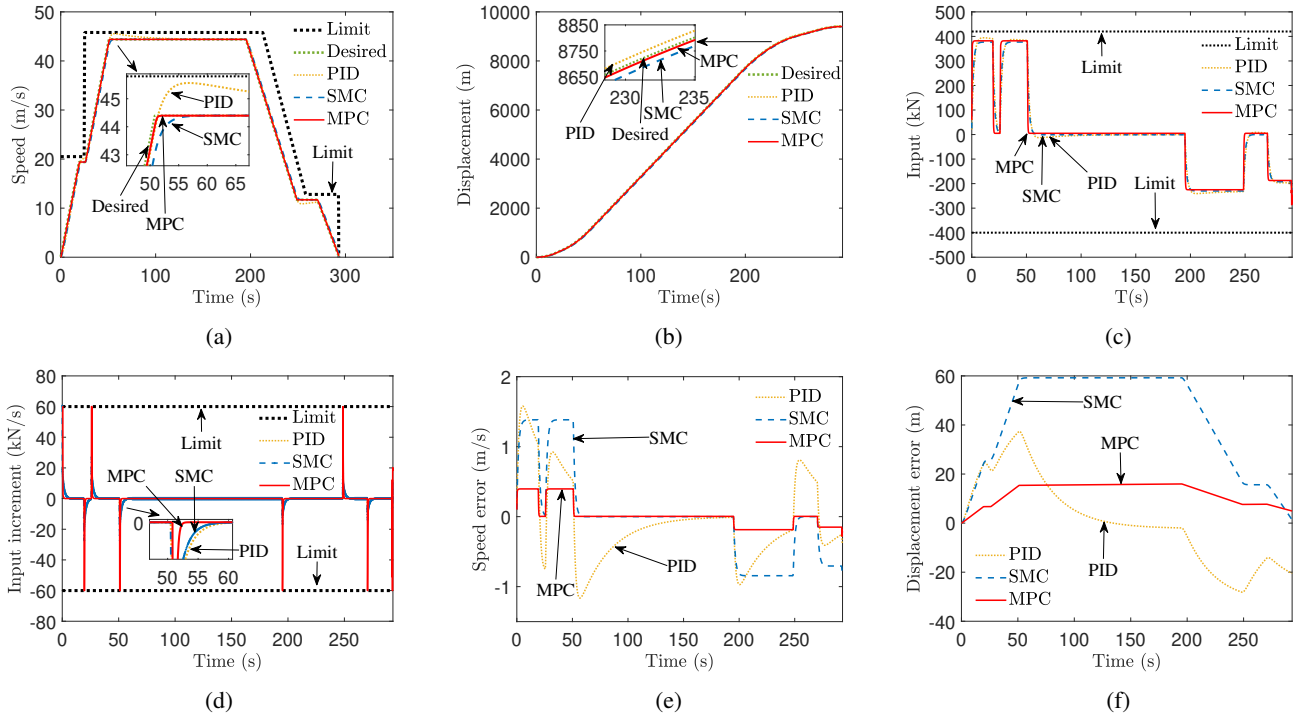

Fig. 4: Comparison of performance in different algorithms without slope resistance.

Figure 3(b) displays the train displacement control performance in different horizons, showing that an increase in prediction and control horizons effectively enhances displacement control accuracy. Figures 3(c) and 3(d) depict the variations in traction/braking force and traction/braking change throughout the train operation. Figure 3(c) reveals that the proposed algorithm can effectively control train speed and displacement within the constraint, meeting the saturation characteristics of the train traction motors. In Fig. 3(d), the traction/braking change, representing riding comfort, remains within the constraint, demonstrating the adaptability of the traction/braking control unit's performance.

Figures 3(e) and 3(f) show the speed error and displacement error during the train operation. It can be observed that an increase in the prediction and control horizons effectively reduces speed error and displacement error, maintaining a speed error of 0.004 m/s during the train cruising phase.

B. Experiment Verification without Slope Resistance

In this section, we explore the differences without slope resistance between the PID-based train speed and displacement control algorithm [9] (referred to as the PID algorithm), the SMC-based train speed and displacement control algorithm [11] (referred to as the SMC algorithm), and the algorithm proposed in this paper, along with their performance in terms of control effectiveness.

Figure 4(a) presents the comparison of train speed control effects for different algorithms, Fig. 4(b) compares the displacement control effects, Fig. 4(c) illustrates the traction/braking effects during the train operation, Fig. 4(d) compares the effects of traction/braking change during the train operation, and Figs. 4(e) and (f) show the speed error and displacement error for different algorithms. The comparative results of the algorithm effects are summarized in Table II.

TABLE II: Performance comparison among different algorithms without slope resistance.

Algorithm	E_u (10^9kN)	E_v (m/s)	E_s (m)
MPC	**9.9033**	**0.1079**	**12.2317**
PID	9.8681	0.4584	13.6817
SMC	9.4185	0.4151	42.8156

As shown in Fig. 4(a), at 55 seconds, the PID algorithm is too close to the speed limit curve, posing a safety hazard with the potential for triggering emergency braking. The SMC algorithm exhibits poorer control performance for tracking the desired speed profile during the train operation. From Fig. 4(b), it is evident that the proposed algorithm closely approximates the desired displacement profile with smaller displacement errors.

Figures 4(c) and 4(d) indicate that, concerning the release of the traction/braking control performance and the balance of riding comfort, this algorithm performs better compared to the other algorithms. As indicated in Table II, the input cost of this algorithm is only increased by 0.35% compared to the PID algorithm and 5.14% compared to the SMC algorithm.

Figures 4(e) and 4(f) show that the speed error and displacement error of the proposed algorithm are smaller on average compared to other algorithms. Combining the results in Table II, the average speed error of the proposed algorithm is approximately 0.25 times that of the PID algorithm and SMC algorithm. The average displacement error can be reduced by 10.6% compared to the PID algorithm and 71.4% compared to the SMC algorithm. In summary, under the constraints of traction/braking force and traction/braking change, the proposed algorithm demonstrates a closer tracking of the

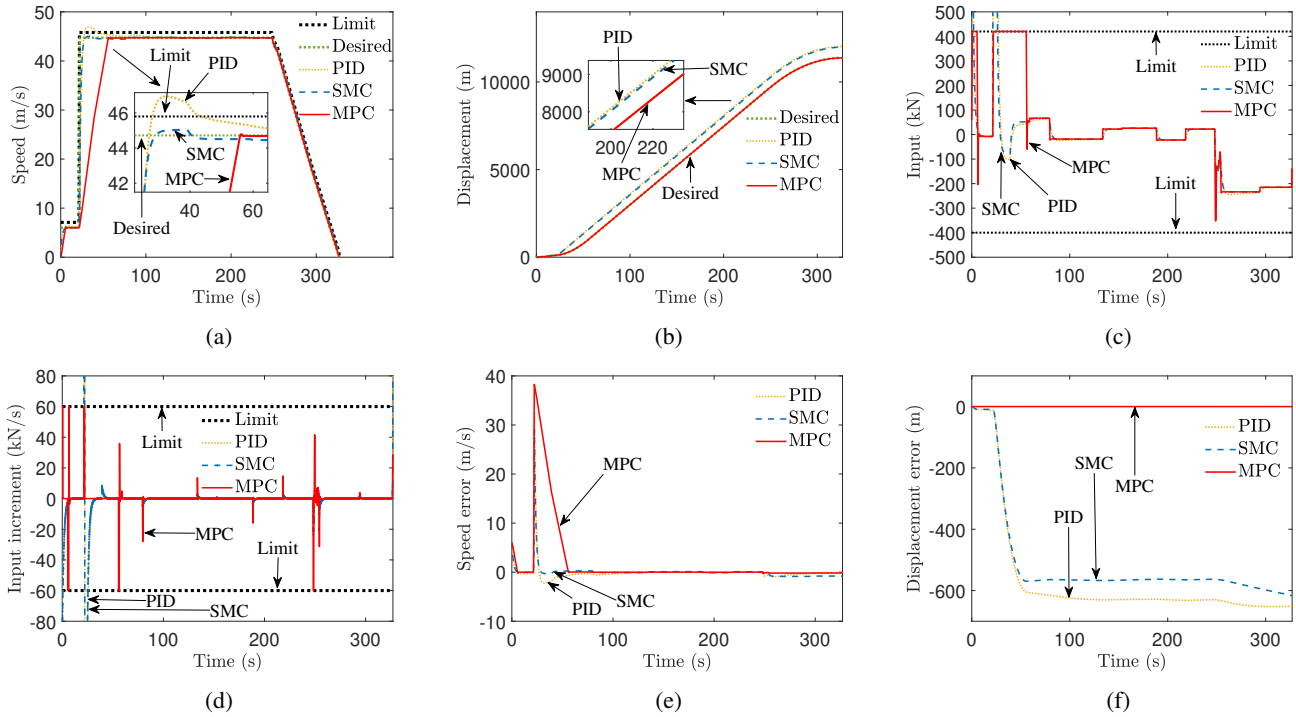

Fig. 5: Comparison of performance in different algorithms with slope resistance.

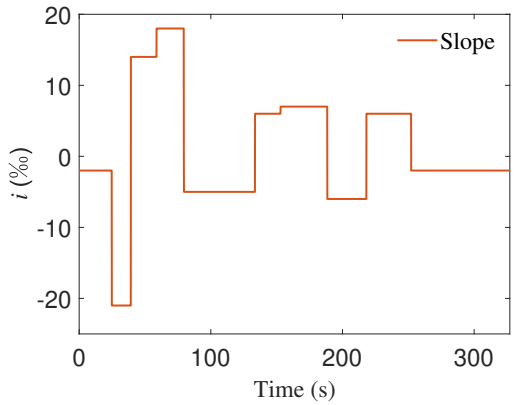

Fig. 6: The slope change in the experiment.

desired profile and superior control performance compared to the PID and SMC algorithms.

C. Experiment Verification with Slope Resistance

Furthermore, the experiment evaluates the control effectiveness in the presence of slope resistance. The change of slope is shown in Fig. 6. Similar to subsection V-B, the comparison of the effects of the proposed algorithm with PID and SMC algorithms is shown in Fig. 5. The comparative results of the algorithm effects are summarized in Table III.

As shown in Fig. 5, when the desired speed profile does not take into account the instantaneous output of the traction motor during the acceleration phase, the PID algorithm and SMC algorithm will have many problems in speed and displacement control. For example, before 35 seconds in Fig. 5(a), although both PID and SMC algorithms can approach the desired profile, such control outputs have exceeded the constraints of traction/braking input. This means that both algorithms do not take riding comfort into account. In contrast, the proposed algorithm can realize the speed and displacement control of the train under multiple constraints, ensuring accurate tracking of the speed and displacement profile.

In Fig. 5(b), compared with the precise tracking of the displacement profile by the MPC algorithm, the other two algorithms exceed the constraint of the speed during the acceleration phase, resulting in huge errors in displacement tracking. In addition, in Figs. 5(c) and (d), corresponding to the control effect in Fig. 5(a), both PID and SMC algorithms exceed the constraint of control input and riding comfort before 35 seconds, while the MPC algorithm achieves precise control within constraints.

Finally, according to Figs. 5(e) and (f), combined with Table III, it can be concluded that the MPC algorithm has a larger average speed error and smaller average displacement error than PID and SMC algorithms. The reason for this is that the other two algorithms do not consider the riding comfort, and they exceed the constraint of the control input increment. In fact, they cannot meet the characteristics of train traction motors.

Overall, as shown in Fig. 5 and Table III, the proposed algorithm can achieve train speed and displacement tracking control while considering slope resistance and multiple constraints.

TABLE III: Performance comparison among different algorithms with slope resistance.

Algorithm	E_u (10^{10}kN)	E_v (m/s)	E_s (m)
MPC	**1.0977**	**1.9911**	**0.0028**
PID	6.2741	0.5432	565.1617
SMC	7.1596	0.4592	513.8754

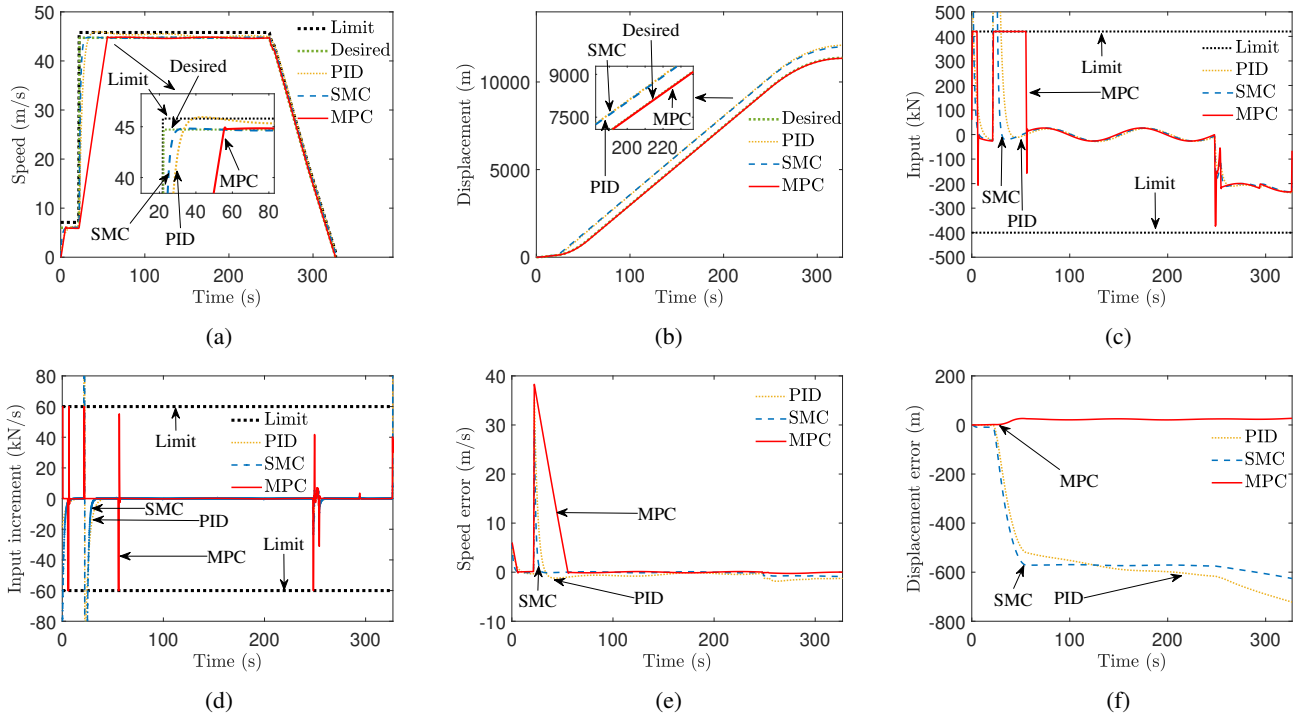

Fig. 7: Comparison of performance in different algorithms with nonlinear disturbance.

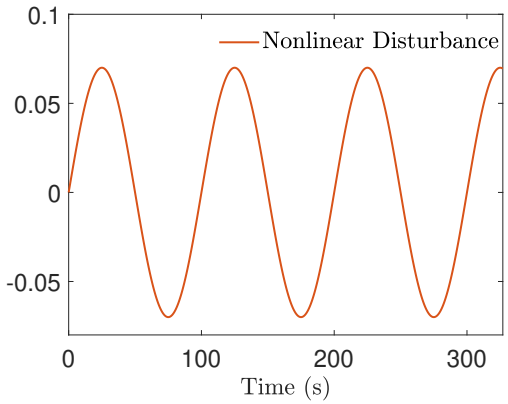

Fig. 8: The nonlinear disturbance in the experiment.

D. Experiment Verification with Nonlinear Disturbance

In this section, the performance of the MPC algorithm with nonlinear disturbance is verified, based on the train operation data in the previous section. The comparison of different algorithms with nonlinear disturbance is shown in Fig. 7. The nonlinear disturbance is shown in Fig. 8. Natural wind is one of the nonlinear disturbances during train operation. Due to the randomness and uncertainty of natural wind, it may affect the operation quality of trains and the stability of the train traction/braking system. According to the natural wind model [30], the following equation describes the characteristics of the nonlinear disturbance.

$$w(t) = 0.07 * \sin\left(\frac{1}{50}\pi t\right),$$

where $w(t)$ represents the nonlinear disturbance.

As shown in Fig. 7 and Table IV, when the train encounters nonlinear disturbance, the performance of the proposed MPC algorithm is better than other algorithms. Note that, in Fig. 7(c), the traction/braking force outputs generated by all three algorithms have corresponding fluctuations due to nonlinear disturbance. However, as shown in the rest subfigures of Fig. 7, the proposed MPC algorithm can still achieve accurate tracking of speed and displacement under constraints of control input and control input increment, and maintain the errors of speed and displacement in a small range. Combined with Table IV, it can be obtained that the proposed MPC algorithm still has excellent control performance of speed and displacement tracking when encountering nonlinear disturbance, which further verifies its benign anti-disturbance performance of the MPC algorithm.

TABLE IV: Performance comparison among different algorithms with nonlinear disturbance.

Algorithm	E_u (10^{10}kN)	E_v (m/s)	E_s (m)
MPC	**1.0483**	**2.1016**	**20.8268**
PID	3.4012	1.1370	534.8395
SMC	7.0675	0.4197	520.1334

VI. Conclusions

This paper has proposed a predictive control algorithm for the speed and displacement tracking of the URT. The proposed algorithm has transformed the ATO control problem into a constrained optimization problem, achieving precise control in various operation scenarios. Experimental results have demonstrated that the proposed algorithm can effectively enhance the speed and displacement control performance while improving energy efficiency, and ensuring safety, stability, and riding comfort. Future research directions will focus on the observation and compensation of unknown disturbances in the operation of the URT.

REFERENCES

[1] X. Yang, X. Li, B. Ning, and T. Tang, "A survey on energy-efficient train operation for urban rail transit," *IEEE Transactions on Intelligent Transportation Systems*, vol. 17, no. 1, pp. 2–13, 2016.

[2] J. Yin, T. Tang, L. Yang, J. Xun, Y. Huang, and Z. Gao, "Research and development of automatic train operation for railway transportation systems: A survey," *Transportation Research Part C: Emerging Technologies*, vol. 85, pp. 548–572, 2017.

[3] H. Dong, X. Gao, Z. Luo, and F. Chang, "Minimum safety distance model based follow operation control of high-speed train," *Engineering Letters*, vol. 26, no. 1, pp. 136 – 142, 2018.

[4] D. Li *et al.*, "Research on energy saving optimization of random traction strategy for urban rail transit," *Engineering Letters*, vol. 31, no. 1, pp. 287 – 294, 2023.

[5] Q. Wu, X. Ge, Q.-L. Han, B. Wang, H. Wu, C. Cole, and M. Spiryagin, "Dynamics and control simulation of railway virtual coupling," *Vehicle System Dynamics*, vol. 61, no. 9, pp. 2292–2316, 2023.

[6] A. Albrecht, P. Howlett, P. Pudney, X. Vu, and P. Zhou, "The key principles of optimal train control—part 2: Existence of an optimal strategy, the local energy minimization principle, uniqueness, computational techniques," *Transportation Research Part B: Methodological*, vol. 94, pp. 509–538, 2016.

[7] W. Lian, B. Liu, W. Li *et al.*, "Automatic operation speed control of high-speed train based on adrc," *Journal of the China Railway Society*, vol. 42, no. 01, pp. 76–81, 2020.

[8] C. Zhang, N. Tan, T. Zhou, M. Liu, and H. Shan, "Research on optimal control of subway train based on fractional order pid controller," *Journal of the China Railway Society*, vol. 40, no. 10, pp. 8–14, 2018.

[9] Q. Pu, X. Zhu, R. Zhang, J. Liu, D. Cai, and G. Fu, "Speed profile tracking by an adaptive controller for subway train based on neural network and pid algorithm," *IEEE Transactions on Vehicular Technology*, vol. 69, no. 10, pp. 10 656–10 667, 2020.

[10] L. Yan, Y. Gao, Z. Yuan, H. Zhao, and S. Gao, "Robust pi protective tracking control of decentralized-power trains with model uncertainties against over-speed and signal passed at danger," *IET Control Theory & Applications*, vol. 15, no. 10, pp. 1314–1334, 2021.

[11] X. Wang, Z. Xiao, M. Chen, P. Sun, Q. Wang, and X. Feng, "Energy-efficient speed profile optimization and sliding mode speed tracking for metros," *Energies*, vol. 13, no. 22, p. 6093, 2020.

[12] Y. Cao, Z.-C. Wang, F. Liu, P. Li, and G. Xie, "Bio-inspired speed curve optimization and sliding mode tracking control for subway trains," *IEEE Transactions on Vehicular Technology*, vol. 68, no. 7, pp. 6331–6342, 2019.

[13] C. Jia, H. Xu, and L. Wang, "Robust nonlinear model predictive control for automatic train operation based on constraint tightening strategy," *Asian Journal of Control*, vol. 24, no. 1, pp. 83–97, 2022.

[14] Z. Wang, Y. Zhou, and D. Liu, "Models and algorithms of conflict detection and scheduling optimization for high-speed train operations based on mpc," *Journal of Control Science and Engineering*, vol. 2018, 2018.

[15] J. Cardenas-Cabrera, L. Diaz-Charris, A. Torres-Carvajal, N. Castro-Charris, E. Romero-Fandiño, J. D. Ruiz Ariza, and J. Jiménez-Cabas, "Model predictive control strategies performance evaluation over a pipeline transportation system," *Journal of Control Science and Engineering*, vol. 2019, pp. 1–11, 2019.

[16] N. Gao, H. Fan, and W. Wu, "A simplified finite control set model predictive control for t-type three-level power conversion system based on lcl filter," *Journal of Control Science and Engineering*, vol. 2021, pp. 1–16, 2021.

[17] Y. Cai, J. Liu, N. Gao *et al.*, "Research on reactive power optimization control method for distribution network with dgs based on improved second-order oscillating pso algorithm," *Journal of Control Science and Engineering*, vol. 2023, 2023.

[18] L. Zhang and X. Zhuan, "Development of an optimal operation approach in the mpc framework for heavy-haul trains," *IEEE Transactions on Intelligent Transportation Systems*, vol. 16, no. 3, pp. 1391–1400, 2014.

[19] L. Wang, H. Xu, C. Zou, and G. Yang, "Application of the model predictive control with constraint tightening for ato system," *International Journal of Control and Automation*, vol. 8, no. 11, pp. 245–262, 2015.

[20] Z. Zhang, H. Song, H. Wang, L. Liu, and H. Dong, "A model predictive control strategy with switching cost functions for cooperative operation of trains," *Science China Information Sciences*, vol. 66, no. 7, p. 172206, 2023.

[21] W. Zhao, J. Ding, Q. Zhang, X. He, and W. Liu, "A distributed multiparticle precise stopping control model based on the distributed model predictive control algorithm for high-speed trains," *Journal of Dynamic Systems, Measurement, and Control*, vol. 145, no. 11, 2023.

[22] J. Felez, Y. Kim, and F. Borrelli, "A model predictive control approach for virtual coupling in railways," *IEEE Transactions on Intelligent Transportation Systems*, vol. 20, no. 7, pp. 2728–2739, 2019.

[23] J. Xun, J. Yin, R. Liu, F. Liu, Y. Zhou, and T. Tang, "Cooperative control of high-speed trains for headway regulation: A self-triggered model predictive control based approach," *Transportation Research Part C: Emerging Technologies*, vol. 102, pp. 106–120, 2019.

[24] S. J. Qin and T. A. Badgwell, "A survey of industrial model predictive control technology," *Control Engineering Practice*, vol. 11, no. 7, pp. 733–764, 2003.

[25] F. Dušek, D. Honc *et al.*, "Desired terminal state concept in model predictive control: A case study," *Journal of Control Science and Engineering*, vol. 2019, 2019.

[26] Y. Liufu, L. Jin, M. Shang, X. Wang, and F.-Y. Wang, "Acp-incorporated perturbation-resistant neural dynamics controller for autonomous vehicles," *IEEE Transactions on Intelligent Vehicles*, pp. 1–12, 2024.

[27] Y. Liufu, L. Jin, and S. Li, "Modified gradient projection neural network for multiset constrained optimization," *IEEE Transactions on Industrial Informatics*, vol. 19, no. 9, pp. 9413–9423, 2023.

[28] J. Kim, J. Park, and Y. Eun, "Precise stop control and experimental validation for metro train overcoming delays and nonlinearities," *IEEE Transactions on Vehicular Technology*, vol. 71, no. 5, pp. 4776–4787, 2022.

[29] C. Jia, H. Xu, and L. Wang, "Nonlinear model predictive control for automatic train operation based on multi-point model," *Journal of Jilin University (Engineering and Technology Edition)*, vol. 50, no. 05, pp. 1913–1922, 2020.

[30] X. Yao, L. Wu, and L. Guo, "Disturbance-observer-based fault tolerant control of high-speed trains: A markovian jump system model approach," *IEEE Transactions on Systems, Man, and Cybernetics: Systems*, vol. 50, no. 4, pp. 1476–1485, 2020.

Xi Wang received the B.S. degree in rail transit signal and control from North University of China, Taiyuan, Shanxi, China, in 2017 and the M.S. degree in information and communication engineering from Inner Mongolia University, Huhhot, Inner Mongolia, China, in 2021. He is currently pursuing a Ph.D. degree in traffic information engineering and control at the China Academy of Railway Sciences, in Beijing, China. His current research interests include automatic train operation, intelligent transportation systems, and model predictive control.

Kejia Xing received the Ph.D. degree in traffic information engineering and control at the China Academy of Railway Sciences, in Beijing, China, in 2004. His current technical title is Researcher. And he guides students' scientific research as a doctoral supervisor. In recent years, he has been engaged in research, standard setting, product development, scientific experiments, and the popularization and application of the next-generation train operation control technology of urban rail transit.

Jian Wang received the B.S. degree in automation from Beijing Jiaotong University, Beijing, China, in 2005, the M.S. degree in traffic information engineering and control, in 2008, and in the Ph.D. program of traffic information engineering and control in China Academy of Railway Sciences. He is currently an Associate Researcher at the Signal and Communication Research Institute, China Academy of Railway Sciences, and an Information Technology Project Management Professional. His research interests include railway signal and communication, and railway intelligent control and dispatching.

Wei Zheng is currently an Associate Researcher at the Signal and Communication Research Institute, China Academy of Railway Sciences Ltd. His research interests include railway signal and communication, and the development of automatic train protection systems.